

## Deuterium retention in tungsten exposed to mixed D+N plasma at divertor relevant fluxes in Magnum-PSI

**H.T. Lee**<sup>\*a</sup>, **G. De Temmerman**<sup>b</sup>,  
**L. Gao**<sup>c</sup>, **T. Schwarz-Selinger**<sup>c</sup>, **G. Meisl**<sup>c</sup>, **T. Höschen**<sup>c</sup>, **Y. Ueda**<sup>a</sup>

<sup>a</sup> Graduate School of Engineering, Osaka University, Suita, Osaka, 565-0871, Japan

<sup>b</sup> Dutch Institute for Fundamental Energy Research, Nieuwegein, 3439 MN, Netherlands

<sup>c</sup> Max-Planck-Institut für Plasmaphysik, D-85748 Garching, Germany

### **Abstract**

Nitrogen (N) has been proposed as an extrinsic impurity species in the divertor to reduce the local power load onto tungsten (W) plasma-facing components. Laboratory studies at low incident fluxes have indicated N increases deuterium (D) retention in tungsten. Here we show that W exposed to D+N Magnum-PSI plasmas under divertor relevant particle fluxes ( $\sim 10^{24}$  D/m<sup>2</sup>s), also results in an increase in D retention by enhanced near surface trapping up to 1100 K due either to N or Mo impurities, and increased retention in the bulk at T > 700 K. These results demonstrate that N or Mo surface impurities have the potential to alter the tritium inventory in tungsten plasma-facing components under diverter relevant particle fluxes by affecting surface and bulk retention processes.

*PACS:* 79.20.Rf, 52.40.Hf, 52.55.Fa, 52.25.Vy

*PSI-21 keywords:* Deuterium inventory, Tungsten, Impurity, Nitrogen

*\*Corresponding author address:* 2-1 Yamada-Oka, Suita, Osaka, Japan.

*\*Corresponding and presenting author E-mail:* heunlee@wakate.frc.eng.osaka-u.ac.jp

*Presenting author:* Heun Tae Lee

## 1. Introduction

In ITER, the foreseen baseline operation is the H-mode. For such a case, 60 to 70 MW of the 100 MW of power entering the divertor must be radiated away [1]. Considering the maximum power load a tungsten (W) plasma-facing component can tolerate is  $<10 \text{ MW/m}^2$ , operation with a partially detached divertor in the inter-ELM period is planned [2]. To meet the radiative power fraction of 60-70%, extrinsic impurities such as nitrogen (N), neon, or argon are being considered in the absence of intrinsic carbon impurities. Nitrogen in particular has received significant interest as an extrinsic impurity [3-5].

The introduction of nitrogen, however, raises issues related to tritium (T) retention in W plasma-facing components. In laboratory studies, N was shown to increase deuterium (D) retention and blistering in W at  $T < 700 \text{ K}$  [6]. Such effects have recently been directly shown to result from an increase in inward diffusion flux by ion driven permeation experiments conducted at low flux [7]. The reason for such an increase is intimately linked with physicochemical changes induced by N implantation at the near surface [7-10]. An increase in bulk diffusion leads to enhanced retention in W and this may pose problems with respect to tritium inventory in the divertor. However, large uncertainty remains in extrapolating laboratory data trends to tokamak experiments due to 3-4 orders of magnitude difference in incident particle fluxes.

This study aims to bridge such a gap by performing experiments using the Magnum-PSI

device [11] relevant to inter-ELM radiative divertor conditions in ITER. The results clearly demonstrate that surface impurities (N or Mo) increases D retention in W due to enhanced trapping at the near surface as well as increased retention in the bulk.

## 2. Experimental

Polycrystalline tungsten specimens (99.99% purity) 20 mm in diameter and hot rolled to 1 mm thickness were prepared by A.L.M.T. Corp, Japan. These specimens were stress relieved at 1573 K for 1 h and polished to a mirror finish on the plasma exposure side. The specimens were installed using the multi-target holder in Magnum-PSI device [12] and exposed to D-only and mixed D+N plasmas in the temperature range 400-1200 K up to a fluence of  $(2-5)\times 10^{25}$  D/m<sup>2</sup>. D-only exposures were performed with source gas flow of 5-6 Pa m<sup>3</sup>/s. D+N exposures were performed by fixing the source D<sub>2</sub>/N<sub>2</sub> gas flow ratio at 12 (D<sub>2</sub>/N<sub>2</sub> flow of 4.8/0.4 or 3.6/0.3 Pa m<sup>3</sup>/s). The pressure in the target chamber was 0.36 Pa during exposures. For most exposures B field of 0.25 T [11] at the target location was used, the only exception being D-only exposures at ~450 K where B field of 0.16 T [11] was used. The bias was -30 V and the pulse length was 12 s for all exposures. Typically, the specimens were exposed to 3 or 4 shots, separated by about 20 minutes to allow for the magnets to cool. Electron density (n<sub>e</sub>) and temperature (T<sub>e</sub>) were measured by Thomson scattering [13] 19 mm upstream from the target specimen. The shot to shot variance was ~10%, which was greater

than the observational error of 3% and 6%, for  $n_e$  and  $T_e$  respectively. Representative  $n_e$  and  $T_e$  measurements are shown for D+N and D-only exposures in Figures 1(a) and 1(b), respectively. It can be seen that the electron density for D+N plasma is approximately twice as high while the temperature does not show the peaked structure as observed in D-only exposures typical for Magnum-PSI [13]. Optical spectroscopy showed a large increase in the N-related signals (320-350 nm) during D+N exposures, while residual N was also observed during D-only exposures when they were conducted after mixed exposures. However, in Section 3.1 we show that the measured N areal densities at the near surface for D-only exposures are comparable to unexposed specimens. Therefore, we conclude that the measured residual N does not play a significant role during D-only exposures.

At present, the absolute N flux incident on the target specimen is unknown. For exposure at  $\sim 800$  K and  $\sim 1100$  K, the gas flow ratio was reduced from 4.8/0.4 to 3.6/0.3 Pa m<sup>3</sup>/s, which did not result in large changes in N-related signal intensities from optical spectroscopy. From this we estimate that the incident N flux was comparable for the two source settings. However, it will be shown that such different settings resulted in a large change in the Mo concentration at the sample surface, which is further discussed in Section 3.

Specimen temperature was controlled by adjusting the thermal contact between the specimen and target holder. Temperature was monitored using a fast thermal camera (FLIR SC7500MB) absolutely calibrated up to 3273 K. The temporal evolution of the temperature at

the specimen center is plotted in Figure 2 for D-only and D+N exposures at: (a) ~450 K (b) ~550 K (c) ~750 K and at (d) ~1100 K only for D+N exposures. The temperature data at ~800 K was not included but was similar to exposures at ~750 K. In general, the specimen reaches steady state temperatures after ~2 s, except for the D-only exposures at ~450 K due to the lower B field. The shot-to-shot variation in temperature at ~450 K and ~550 K is less than 20 K, while at ~750 K the difference increases to 100 K and 50 K for D+N and D-only exposures, respectively. Temperature control was poorest for exposures at ~1100 K where temperature difference ranges from 200-400 K. In section 3, the N and D retention results are plotted as function of temperature at 7 s, averaged over 3-4 shots, while the error represents the standard deviation in temperature for all shots combined. The temperature variation across the specimen for a given shot was much smaller compared to the difference between shots. Following exposures, no mass loss was discernable within  $\pm 0.05$  mg.

The *near surface* N areal density (<100 nm) was determined by  ${}^4\text{He}$  nuclear reaction analysis (NRA) using the reaction  ${}^{14}\text{N} ({}^4\text{He}, \text{p}^0) {}^{17}\text{O}$  [14], at incident  ${}^4\text{He}$  ion energy of 4.8 MeV. The scattering angle was  $135^\circ$  with a detector solid angle of 29.94 msr. The measurements were performed at three different spots (center and  $\pm 1$  mm). The different N locations were chosen to check for analysis beam induced depletion effects. It was found that the N areal density varied by no more than 20%. The N areal density presented in Figure 3 corresponds to the average of all three measurements. N concentration was determined by

integrating the spectrum and comparison to a calibration target of known N areal density.

However, the near surface N depth profile could not be determined due to the unknown stopping power of the mixed near surface layer.

D retention was investigated by  $^3\text{He}$  nuclear reaction analysis following procedures similar to Mayer et al. [15]. NRA measurements were performed at three different spots (center and  $\pm 4$  mm). The different D locations were chosen to check for variation that may arise due to the non-uniformity of the plasma exposure conditions across the specimen surface. The D concentration varied between 20-200 % depending on the analysis location. Therefore, the average D concentrations from the three measurements are presented in Figure 5, while only the D depth profiles from the center measurements are presented in Figure 6 due to space constraints. The near surface D areal density was determined from  $\text{D}(^3\text{He}, ^4\text{He}) \text{ p}^0$  [15] reaction using the  $102^\circ$  detector at incident He ion energy of 0.69 MeV. D depth profiles up to 8  $\mu\text{m}$  were determined by collecting the protons with a  $135^\circ$  detector (solid angle of 29.94 msr). The incident  $^3\text{He}^+$  ion energies used were 0.69, 1.2, 1.8, 2.4, 3.2 and 4.5 MeV. Typically, 10  $\mu\text{C}$  was collected for each measurement. The most probable D depth profiles were determined by deconvolution using the program NRADC [16].

X-ray photoelectron spectroscopy (XPS) depth profiles were measured in a PHI 5600 ESCA system using a standard Al K X-ray source and 10 keV Ar ions for sputtering. The peak intensities were derived from the measured spectra by Shirley background subtraction

and the N 1s peak intensity was separated from the nearby Mo 3p peak by a fitting procedure.

The given concentrations in Figure 4 were calculated from the peak intensities via relative sensitivity factors.

### 3. Results and discussion

#### 3.1. Near surface N and D retention

The N-areal density for D-only and mixed D+N exposures are plotted as function of exposure temperature in Figure 3 in square and circle symbols, respectively. For D-only exposures at  $T > 450$  K, the N areal density was similar to levels measured from an unexposed sample surface (indicated by dotted line) which is representative of N contamination following transport through air. At  $T \sim 450$  K, a threefold increase in the N areal density was observed. We attribute such change to a difference in the exposure history. Prior to the D-only exposure at  $\sim 450$  K, a combined twelve D+N shots were performed in comparison to three D+N shots at the higher temperatures. The increased number of shots likely resulted in an increase in N contamination of the source and target chamber leading to the observed increase in N areal density levels similar to D+N exposure.

For D+N exposures, an increase in the N areal density in comparison to D-only exposures was observed at  $T > 450$  K. However, no clear temperature dependence was observed. Specifically, a sevenfold increase in N areal density at  $\sim 800$  K was observed as

indicated by the arrow in Figure 3. This large difference in N areal density seemed to result from the different source D<sub>2</sub>/N<sub>2</sub> gas flow ratio used, as indicated by the open and closed symbols (circle), corresponding to D<sub>2</sub>/N<sub>2</sub> gas flow ratio of 3.6/0.3 and 4.8/0.4 Pa m<sup>3</sup>/s, respectively. In Figure 4, the surface N and Mo concentrations are plotted as a function of sputter time for the two different source conditions at ~800 K. Also shown in the secondary x-axis is an estimate of the depth scale by assuming a constant sputter yield of 2, which is reasonable for W, but is an underestimate of the Mo or N. The N concentration closely followed the Mo concentration and an increase in the Mo concentration was observed when the source D<sub>2</sub>/N<sub>2</sub> gas flow changes from 4.8/0.4 to 3.6/0.3 Pa m<sup>3</sup>/s. This suggests that the absolute N concentration is closely linked to the Mo concentration, and the increase in N concentration at ~800 K and ~1100 K may be due to co-deposition with Mo impurities. However, it could not be concluded from present XPS measurements if molybdenum nitrides were formed due to the non-ambiguous positions of the peaks.

The D areal density at the near surface for mixed D+N exposures is plotted in Figure 5 (a) as function of temperature along with N areal density from Figure 3. Again, the solid and open symbols correspond to source D<sub>2</sub>/N<sub>2</sub> gas flow ratio of 3.6/0.3 and 4.8/0.4 Pa m<sup>3</sup>/s, respectively. First, the D areal density showed similar temperature dependence to N areal density. Second, the measured D areal density represents a large increase in D retention, since the D areal density from D-only exposures were below the detection limit of measurements.

From Figure 5 (a), by assuming that all the D was trapped with N, the ratio of trapped D to N concentration at the near surface can be estimated and is plotted in Figure 5 (b). The D/N ratio showed a maximum at  $\sim$  800 K, which is the temperature at which tungsten nitrides have been observed to decompose in laboratory experiments [14]. However, it is also known that molybdenum nitride ( $\text{Mo}_2\text{N}$ ) decomposes at similar temperatures [17]. In Figure 5 (c), the ratio of trapped D/Mo is plotted as function of temperature. This ratio was determined by multiplying the D/N ratio from Figure 5 (b) with the N/Mo concentration ratio at the surface in Figure 4 (the average value of the first two measurements were taken). The D/Mo ratio also showed a decrease in the temperature interval where the  $\text{Mo}_2\text{N}$  decomposes. Therefore, we cannot at present distinguish if the increase in D retention at the near surface following mixed D+N exposures arise from D trapping with N, Mo, or its combined effect, and more controlled laboratory experiments are required.

To gain some insight into the dominant process, the steady state permeation flux during D+N irradiation (open diamond symbols) from a separate experiment conducted at low flux [7] without Mo impurity contamination is plotted in Figure 5 (b). The line is meant to guide the eye only. It can be seen that the permeation flux and the D/N ratio followed a similar temperature dependency within the error of temperature measurements. This suggests that the near surface trapped D concentration may also be responsible for controlling the solute D concentration. Consequently, N induced changes to the near surface establishes the boundary

condition for inward D diffusion flux into the bulk, which controls both the rate and total D retention in W as discussed further in Section 3.2 below.

### 3.2. D retention up to 8 $\mu\text{m}$

D depth profiles are plotted in Figure 6 at (a)  $\sim 450$  K, (b)  $\sim 550$  K, and (c)  $\sim 750 / \sim 800$  K for mixed D+N exposures and  $\sim 750$  K for D-only exposures. Also plotted in Figure 6 (c) is D depth profile at  $\sim 1100$  K for mixed D+N exposures. From Figure 6 (a) and (b), it can be seen that for surface temperatures below 550 K the effect of nitrogen on D trapped up to 8  $\mu\text{m}$  is limited, aside from the increase in near surface D as discussed already in Section 3.1. Such results are in qualitative disagreement with sequential N and D laboratory experiments [9] where enhanced D trapping was observed at depths of 1-5  $\mu\text{m}$ . An increase in D retention at such depth generally corresponds to typical depths where distortion and cracking is observed [18] resulting in blistering of W surface. Perhaps the discrepancy results from the fact that D-only exposures at fluxes typical in Magnum-PSI ( $\sim 10^{24} \text{ D/m}^2\text{s}$ ) already result in significant increase in D retention at depths up to 1  $\mu\text{m}$  in comparison to laboratory experiments at lower fluxes [19]. This is postulated to arise from stress-induced effects due to the high fluxes. Therefore, such stress-induced effects may already dominate at D-only exposures, and the influence of nitrogen-induced increase in inward diffusion flux may be limited at divertor relevant particle fluxes at  $T < 750$  K.

At  $T \sim 750$  K, an order of magnitude increase in retention was observed for D+N exposure in comparison to D-only exposure as seen from Figure 6 (c). Permeation experiments [7] have shown an order of magnitude increase in permeation flux at  $T \sim 700$  K, which semi-quantitatively can explain the observed increase in trapped amount by invoking the argument of local equilibrium between trapped and solute concentrations. However, at  $\sim 800$  K the trapped D-concentration at the near surface was two orders of magnitude higher, while no difference in the trapped amount in the bulk was seen. This apparent contradiction can be resolved if we consider the traps are saturated within the depth probed by NRA measurements, and the D depth profile at depths greater than 8  $\mu\text{m}$  needs to be known to determine if the penetration depth is deeper for the case of  $\sim 800$  K exposures.

At  $T \sim 1100$  K, D retention was still observed as shown in Figure 6 (c). This is a surprising result and may pose a concern with respect to T inventory. At present, it is unclear if D retention at such high temperature occurs due to N or Mo, and if such impurities inhibit the outward release of D, resulting in previously mobile D to become trapped as the specimen cools following exposures. If such a process is indeed valid, then this is an important aspect to consider for all fusion devices operating in pulsed mode in the presence of N- or Mo-impurities (e.g. from Inconel), since the kinetics of hydrogen diffusion/release may compete against cooling/heating cycles.

#### **4. Summary**

The influence of nitrogen on D retention at divertor relevant particle fluxes has been studied by mixed D+N and D-only plasma exposures using Magnum-PSI. The effect of N on D trapping and transport could not be unambiguously determined due to complications arising from the presence of Mo impurities at the surface. The experimental findings and discussion can be summarized as follows:

- At near surface ( $< 100$  nm) : N trapping was weakly temperature dependent with N still present at  $T > 750$  K. The trapped N and Mo concentrations followed similar depth distributions and such N or Mo induced changes to the near surface was responsible for the increased D retention during mixed D+N exposures. The trapped D/N ratios follow similar temperature dependence to steady state permeation fluxes from a separate experiment at low flux [7] suggesting that the D trapped with N or Mo, may also control the inward bulk diffusion flux.
- At bulk (up to  $8 \mu\text{m}$ ) : N or Mo impurities did not significantly alter the trapped D depth profiles at  $T < 750$  K, while an order of magnitude increase was observed at  $T \sim 750/800$  K, which was interpreted to arise from an order of magnitude increase in solute D concentration. D retention was observed at  $T \sim 1100$  K, which was interpreted to arise from combined effect of slow kinetics of D release from the surface due to the presence of N or Mo impurities combined with rapid cooling of the specimen.

## **Acknowledgements**

This work was supported in part by TEXTOR-Japan international collaboration. Magnum-PSI operation by J. Scholten and technical assistance of M.A van den Berg with temperature measurements are gratefully acknowledged. The technical support of M. Fueßeder and J. Dorner with NRA measurements are also gratefully acknowledged.

## References

- [1] R.A. Pitts, A. Kukushkin, A. Loarte, A. Martin, M. Merola, C.E. Kessel, et al., Phys. Scr. T138 (2009) 014001.
- [2] A. Loarte, J.W. Hughes, M.L. Reinke, J.L. Terry, B. LaBombard, D. Brunner, et al., Physics of Plasmas 18 (2011) 056105.
- [3] A. Kallenbach, M. Balden, R. Dux, T. Eich, C. Giroud, A. Huber, et al., Journal of Nuclear Materials 415 (2011) S19–S26.
- [4] C. Giroud, G.P. Maddison, S. Jachmich, F. Rimini, M.N.A. Beurskens, I. Balboa et al., Nucl. Fusion 53 (2013) 113025.
- [5] M. Oberkofler, D. Douai, S. Brezinsek, J.W. Coenen, T. Dittmar, A. Drenik et al., Journal of Nuclear Materials 438 (2013) S258-261.
- [6] O.V. Ogorodnikova, K. Sugiyama, A. Markin, Yu. Gasparyan, V. Efimov, A. Manhard et al., Phys. Scr. T145 (2011) 014034.
- [7] H.T. Lee, M. Ishida, Y. Ohtsuka, and Y. Ueda, Phys. Scr. T159 (2014) 014021.
- [8] L. Gao, W. Jacob, T. Schwarz-Selinger, and A. Manhard, Journal of Nuclear Materials, 451 (2014) 352–355.
- [9] L. Gao, W. Jacob, P. Wang, U. von Toussaint, and A. Manhard, Phys. Scr. T159 (2014) 014023.
- [10] K. Schmid, A. Manhard, Ch. Linsmeier, A. Wiltner, T. Schwarz-Selinger, W. Jacob, et al. Nucl. Fusion 50 (2010) 025006.

- [11] J. Scholten, P.A. Zeijlmans van Emmichoven, H.J.N. van Eck, P.H.M. Smeets, G.C. De Temmerman, S. Brons, et al., *Fusion Eng. and Design* 88 (2013) 1785-1788.
- [12] G. De Temmerman, M.A. van den Berg, J. Scholten, A. Lof, H.J. van der Meiden, H.J.N. van Eck et al., *Fusion Engineering and Design* 88 (2013) 483-487.
- [13] H. J. van der Meiden, M.A. van den Berg, S. Brons, H. Ding, H.J.N. van Eck, M.H.J ‘t Hoen, et al., *Journal of Instrumentation* 8 (2013) C11011.
- [14] G Meisl, K Schmid, O Encke, T Höschen, L Gao and Ch Linsmeier, *New J. Phys.* **16** (2014) 093018.
- [15] M. Mayer, E. Gauthier, K. Sugiyama and U. von Toussaint, *Nucl. Instr. Meth. Phys. Res. B* 267 (2009) 506-512.
- [16] K. Schmid and U. von Toussaint, *Nucl. Instr. Meth. Phys. Res. B* 281(2012) 64-71.
- [17] Z. Wei, Q. Xin, P. Grange, and B. Delmon, *Journal of Catalysis* 168 (1997) 176-182.
- [18] S. Lindig, M. Balden, V.Kh. Alimov, T. Yamanishi, W.M. Shu, and J. Roth, *Phys. Scr.* T138 (2009) 014040.
- [19] L. Buzi, G. De Temmerman, B. Unterberg, A. Litnovsky, V. Philipps, G. Van Oost<sup>1</sup>, et al., “Influence of particle flux density and temperature on surface modifications of tungsten and deuterium retention”, *Journal of Nuclear Materials* (2014) submitted.

## Figure captions

Figure 1: Typical plasma properties: (a) density and (b) temperature for mixed D+N and D-only plasmas determined by Thomson scattering. The source gas flow was  $5 \text{ Pa m}^3/\text{s}$  for D-only exposures, and  $\text{D}_2/\text{N}_2$  flow of  $4.8/0.4 \text{ Pa m}^3/\text{s}$  for D+N exposures. The B field was  $0.25 \text{ T}$ , the bias was  $-30 \text{ V}$ , and the pulse length was  $12 \text{ s}$  for all exposures.

Figure 2: Specimen temperature as function of time at the specimen center for D+N and D-only exposures showing the shot-to-shot variance.

Figure 3: NRA measurements showing near surface N areal density as function of temperature for D+N and D-only exposures. For D-only exposures, the crossed square symbol at  $\sim 450 \text{ K}$  correspond to exposures following 12 D+N shots, while the solid squares correspond to exposures following 3 D+N shots. The dotted line indicates representative N contamination levels due to specimen transport in air. For D+N exposures, the open and closed symbol correspond to the different source conditions used ( $\text{D}_2/\text{N}_2$  gas flow ratio of  $4.8/0.4$  or  $3.6/0.3 \text{ Pa m}^3/\text{s}$ ), with the change in N areal density indicated by the arrow.

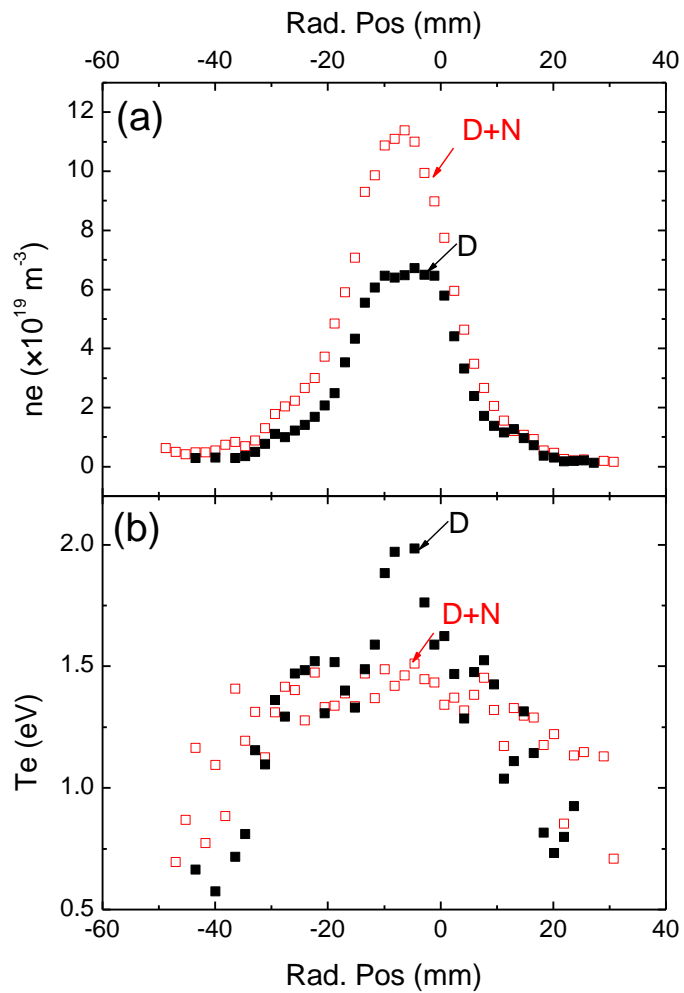
Figure 4: Nitrogen and molybdenum concentrations as function of sputter time from XPS for two D+N exposed samples at  $\sim 750 \text{ K}$  and  $\sim 800 \text{ K}$  with source  $\text{D}_2/\text{N}_2$  gas flow ratio of  $4.8/0.4$

or  $3.6/0.3 \text{ Pa m}^3/\text{s}$ , respectively. The secondary x-axis was calculated assuming a constant sputter yield of 2, which is an underestimate of N or Mo.

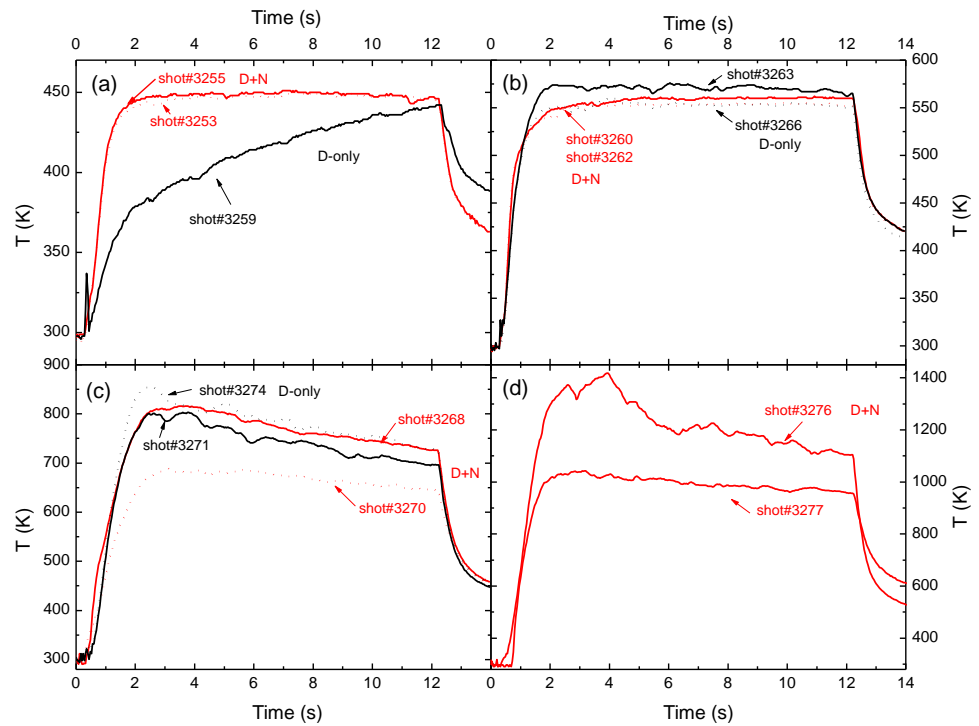
Figure 5: (a) NRA measurements showing near surface D or N areal density as function of temperature for D+N exposed samples; (b) D/N ratio determined from (a) plotted as function of temperature. Also plotted are steady state D permeation flux during mixed D+N irradiation using a low flux ion beam experiment [7]; (c) D/Mo ratio determined by multiplying the D/N ratio from (b) with the surface N/Mo ratio in Figure 4.

Figure 6: NRA depth profiles showing D trapping up to  $8 \mu\text{m}$  for D+N and D-only exposures at (a)  $\sim 450 \text{ K}$ ; (b)  $\sim 550 \text{ K}$ ; and (c)  $\sim 750 \text{ K}$  and  $\sim 800 \text{ K}$ . Also plotted is D+N exposure at  $\sim 1100 \text{ K}$ . The lines are meant to guide the eye-only.

**Figure 1 (one column)**



**Figure 2 (one column)**



**Figure 3** (one column)

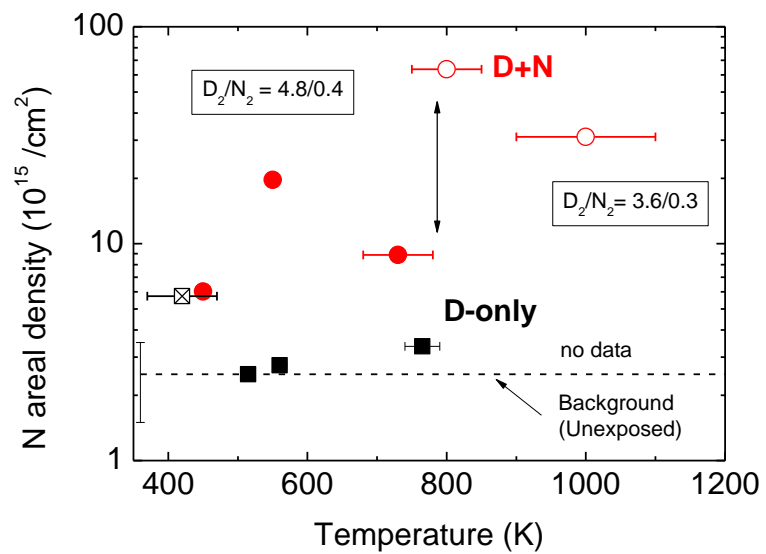


**Figure 4** (one column)

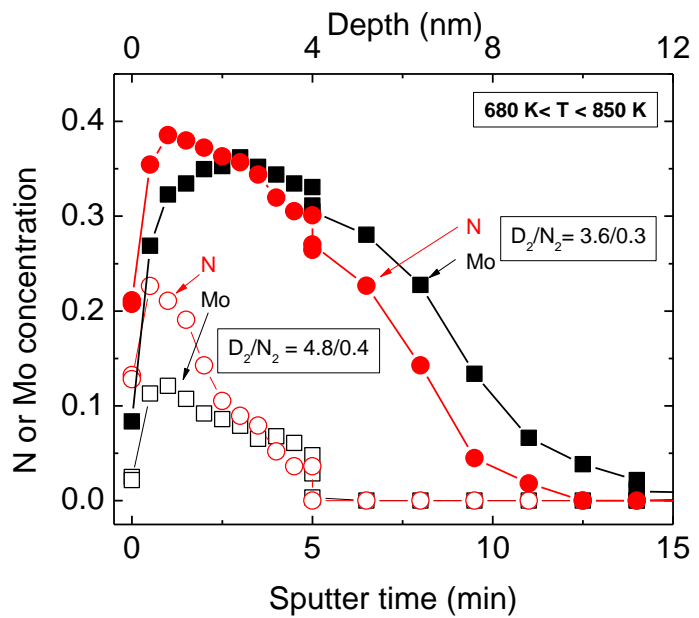


**Figure 5** (one

column)

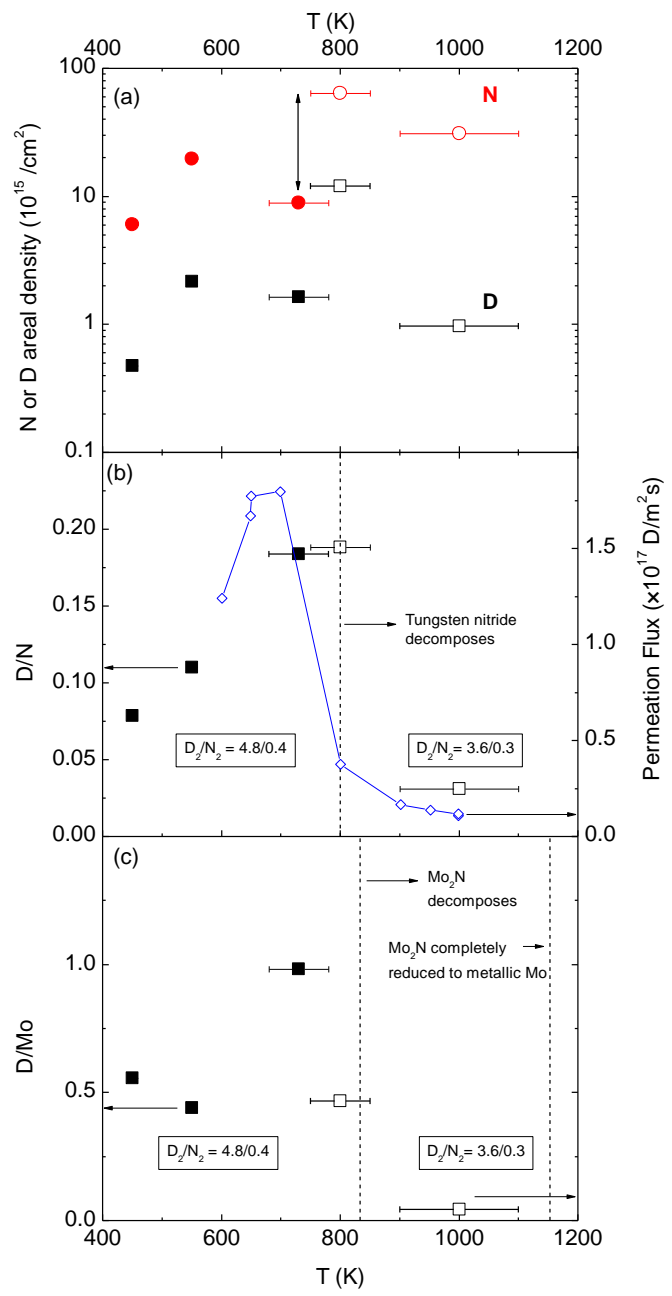


**Figure 6 (one column)**

